doi: 10.56761/EFRE2022.C3-P-012501

# Evolution of the structure and properties of AISI 1020 steel subjected to elion nitriding in a low-pressure gas discharge plasma

*I.V. Lopatin*, Yu.H. Akhmadeev, E.A. Petrikova, M.E. Rygina, Yu.F. Ivanov*

*Institute of High Current Electronics SB RAS, Tomsk, Russia*
**lopatin@opee.hcei.tsc.ru*

**Abstract.** A method and experiments of nitriding AISI 1020 steel with simultaneous heating of the samples with the electron component of plasma are described. A nitriding regime is explained that makes it possible to form a hardened layer up to 500 μm thick. It is shown that the microhardness of the surface layer of the steel increases with the increase in the nitriding temperature and correlates with the relative content of the nitride phase. It has found that in the nitriding temperature range from 450 °C to 600 °C, the maximum microhardness is formed in the near-surface layer at the depth of ~10 μm at 520 °C. It has been established that the steel wear resistance is determined by the concentration of nitrogen atoms in the α-Fe crystal lattice. It has been shown that micropores formed in the surface layer of the steel nitrided at 520 °C contribute to an increase in material wear under dry friction.

**Keywords:** structural steel, gas discharge plasma, ion-electron method, nitriding, structure, properties.

## 1. Introduction

The state and properties of the surface layer of a product material often define the product operational characteristics. Long-term studies show the possibility and relevance of modifying the surface of metals and alloys by saturating the surface layer with atoms of gas elements, e.g. nitrogen. This treatment is called nitriding [1–3]. Nitriding is accompanied by the formation of a gradient structure in the near-surface layer where the concentration of alloying atoms changes in the depth profile [4–6], which makes it possible to significantly increase the hardness and wear resistance, corrosion resistance and electrical conductivity (etc.) of the surface. At the same time, the structure of the modified layer, its phase composition, strength and tribological characteristics are largely determined by the chemical and phase composition of steel. For example, it is known that the presence of even up to 1% chromium affects the surface phase composition of steels and the depth profile of both nitrogen and microhardness [5]. It is further know that the depth profile of nitrogen and microhardness becomes non-monotonic after processing stainless austenitic steels where the concentrations of alloying elements, such as chromium and nickel, amount to tens of percent, due to the difficult penetration of nitrogen atoms into samples and simultaneous intensive formation of nitrides of alloying elements in near-surface layers. Thus, in order to understand nitrogen diffusion, it is of interest to study industrial steels that are free from nitride-forming additives.

Beside the composition of such steels, nitriding conditions are important factors that can influence the profile and properties of the modified layers. In case of ion-plasma nitriding, nitriding occurs in the presence of nitrogen in the ionized state [7–10]; therefore, the intensity of ion exposure on the treated surface during nitriding should be considered. At the same time, the intensity of ion exposure is related to the nitriding temperature, which, in turn, also significantly affects the formation of the modified layer. To reduce the influence of the intensity of ion exposure on the formation of the modified layer, it was proposed in [11, 12] to use the electron components of plasma (elion processing) to heat the samples, which makes it possible to change the processing temperature without significantly changing the intensity of ion bombardment of the samples.

This article describes the structure and properties of AISI 1020 steel (which has insignificant number of nitride-forming components) subjected to elion nitriding at identical density and energy of nitrogen ions and at different processing temperatures.

## 2. Materials and methods

Nitriding was carried out in the plasma of a non-self-sustained arc discharge with a heated cathode generated by a source of our own design [13, 14]. The design of the discharge power supply and substrate bias system makes it possible to use the electron component of plasma to heat samples in the intervals between ion cleanings. The experimental setup is described in detail in [11, 12, 15].

Steel St20 (analogous to AISI 1020 steel) of elemental composition (wt. %) (0.17–0.24)C--(0.17–0.37)Si-(0.35–0.65)Mn-(to 0.25)Cr-(to 0.3)Ni-(to 0.3)Cu-(to 0.04)S-(to 0.035)P-(the rest Fe) was used in the experiments. The samples had the shape of cylinders ∅25×5 mm in size polished on one side. Nitriding was carried out in a gas discharge plasma at temperatures 450, 520 and 600 °C for 2 hours with the following settings: nitrogen pressure 0.6 Pa; discharge current of the PINK plasma generator 40 A; discharge voltage of the PINK plasma generator 60 V; time fraction of electron heating of samples 15% (at nitriding temperature 450 °C), 25 % (at 520 °C) and 39% (at 600 °C); bias voltage of the substrate during ion cleaning of the sample surface 300 V. The surface of the samples was cleaned with nitrogen ions with the bias voltage of 700 V for 10 minutes before nitriding. After nitriding the samples were cooled in the vacuum chamber to some temperature below 100 °C at a pressure of at least $1 \cdot 10^{-3}$ Pa. The phase composition of the steel was studied by X-ray diffraction analysis. The structure of the nitriding surface and the elemental composition of the surface layer were analyzed by scanning electron microscopy. The defective substructure and phase composition of the surface layer up to 50 μm thick were studied by transmission electron diffraction microscopy of thin foils. The foils were made from plates cut in the cross section of the bulk sample. The mechanical properties of the steel were characterized by microhardness (at indenter load 0.5 N and 1 N). The tribological properties were characterized by wear (inversely proportional to wear resistance) and friction coefficient.

## 3. Research results and discussion

Scanning electron microscopy was used to study the surface structure formed during nitriding. It was found that nitriding was accompanied by the formation of a submicro-nanocrystalline structure in the surface layer. The crystallite size increased from 60 nm (Fig.1b) to 330 nm (Fig.1f) with the increase in the nitriding temperature from 450 to 600 °C. It should be noted that nitriding at 520 °C was accompanied by the formation of micropores of 100–200 nm in the surface layer (Fig.1d).

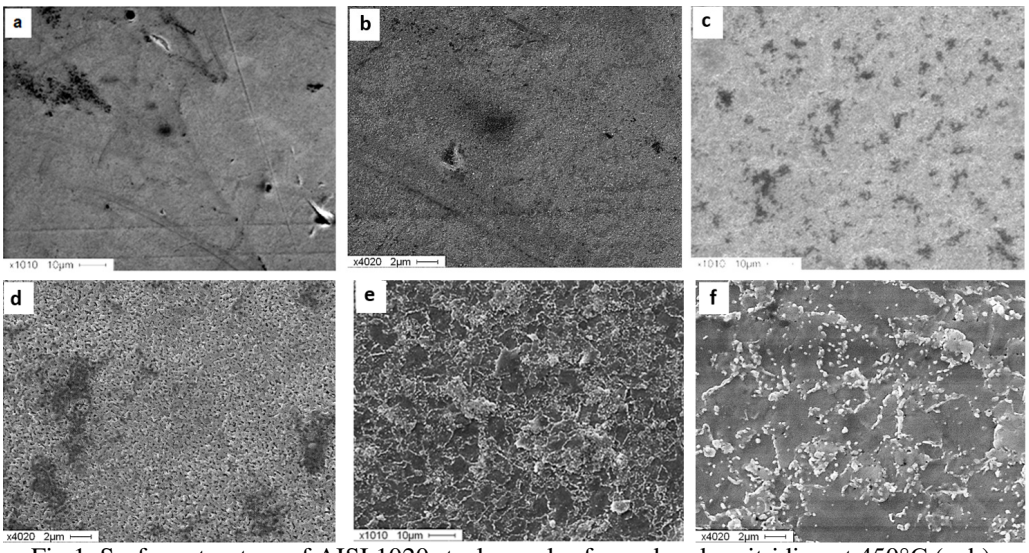


Fig.1. Surface structure of AISI 1020 steel samples formed under nitriding at 450°C (a, b); 520 °C (c, d) and 600 °C (e, f); scanning electron microscopy.

The elemental composition of the surface layer was studied by X-ray microanalysis. It was found (by area) that the concentration of nitrogen in the surface layer of the steel varied non-monotonically and reached the minimal value of 13.5 at.% at the nitriding temperature 520 °C (Fig.2).

Elemental analysis of individual crystallites made it possible to record the inhomogeneity of the distribution of nitrogen atoms within an individual sample. The results in Fig.3 show that the surface layer contains both nitrogen-enriched crystallites and nitrogen-depleted crystallites (Table 1). At the same time, nitrogen concentration in the areas of light contrast (Fig.3, indicated in (a) with the "+" sign and the digit "1") is higher compared to the dark contrast areas (Fig.3, indicated in (a) with the "+" sign and the digit "2").

**Table 1.** X-ray microanalysis of areas 1 and 2 indicated in Fig.3a

| Analyzed areas | **N, at. %** | **Fe, at. %** |
|---|---|---|
| 1 | 14.7 | 85.3 |
| 2 | 10.2 | 89.8 |

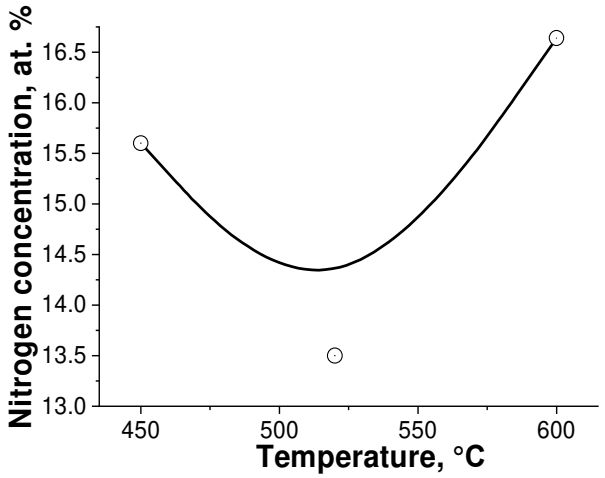


Fig.2. Dependence of nitrogen concentration in the surface layer of AISI 1020 steel on nitriding temperature.

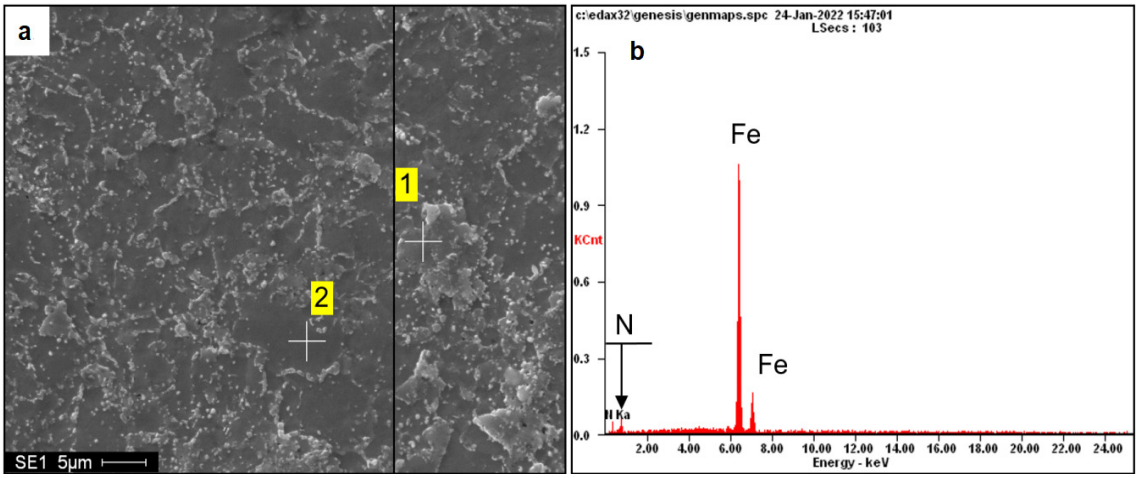


Fig.3. Electron microscope image of the surface structure of AISI 1020 steel nitrided at 600 °C(a); b – energy spectra in the area indicated in (a) by the "+" sign and the digit "1".

X-ray phase analysis was used to find significant transformation of the phase composition of the steel surface layer during nitriding (Fig.4 and Fig.5). For example, a solid solution based on α-

Fe (97 wt. %) was the main phase in the surface layer after nitriding at 450°C (Fig.4, X-ray image 1, Fig.5a), while $Fe_4N$ was the main phase in the surface layer after nitriding at 520 and 600 °C (Fig.4, X-ray image 2).

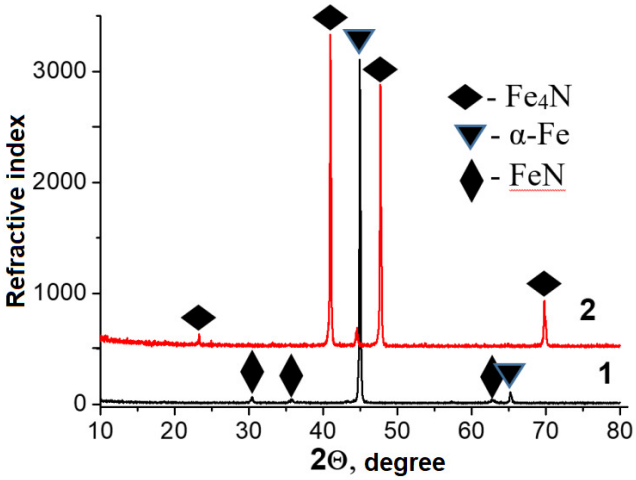


Fig.4. X-ray images of AISI 1020 steel samples nitrided at 450 °C (1) and 600 °C (2).

Simultaneously with the change in the phase composition of the steel surface layer, the parameter of the α-Fe crystal structure also changed. The results in Fig.5b indicate that the lattice parameter of α-Fe changes nonmonotonically and reaches its maximum value at the nitriding temperature of 520 °C. The results in Fig.6 indicate that there is a weak correlation between the lattice parameter of α-Fe and the nitrogen concentration in steel, which does not allow making an unambiguous link between the change in the steel lattice parameter and the nitrogen concentration in the material.

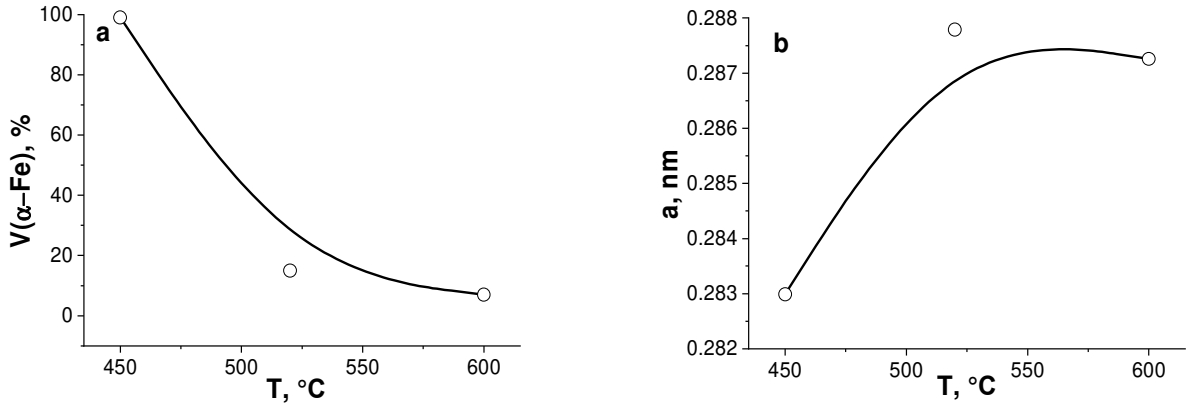


Fig.5. Dependence of the relative content of α-Fe (a) and the lattice parameter of α-Fe (b) on the temperature of nitriding AISI 1020 steel.

The microhardness of the nitrided steel is shown in Fig.6. It can be clearly seen that an increase in the nitriding temperature is accompanied by an increase in the microhardness of the surface layer up to 8.9 GPa at the nitriding temperature of 600 °C. Comparison of the results in Fig.5a and Fig.6 demonstrate that the hardness of the surface layer increases with the increase in the relative content of the nitride phase in the material.

Fig.7 shows the microhardness of AISI 1020 steel depending on the distance from the nitrided surface. It can be clearly seen that the microhardness profile greatly depends on the nitriding temperature. The maximum microhardness was recorded on the nitriding surface at 450 °C and

600 °C (Fig.6); at the depth of ~10 μm at 520 °C. Apparently, this is due to the formation of a microporous structure in the steel surface layer during nitriding at 520 °C (Fig.1c). The greatest thickness of the hardened layer (up to 500 μm) was achieved after nitriding at 520 °C. The samples nitrided at this temperature demonstrated a gradual decrease in microhardness at growing distance from the treated surface.

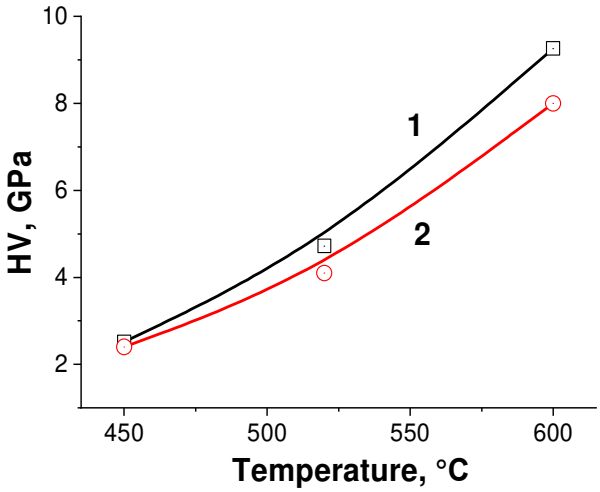


Fig.6. Dependence of the microhardness of the surface layer of the AISI 1020 steel on the nitriding temperature; indenter load: 1 – 0.5 H; 2 – 1 H. The hardness of AISI 1020 steel in the initial state was 1.9 GPa.

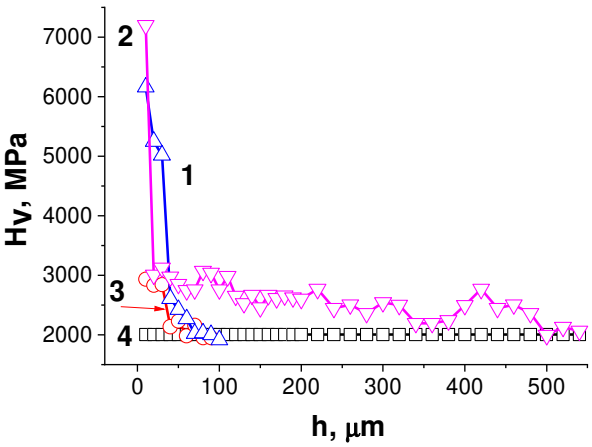


Fig.7. Microhardness profiles of AISI 1020 steel nitrided at 600 °C (curve 1), 520 °C (curve 2), and 450 °C (curve 3); curve 4 – AISI 1020 steel in its initial state.

## 4. Conclusion

Samples of AISI 1020 steel were subjected to elion nitriding, which ensured efficient heating of the samples by the electron component of plasma. It has been found (by X-ray microanalysis) that the concentration of nitrogen in the steel surface layer varied nonmonotonically and reached the minimal value of 13.5 at. % at the nitriding temperature 520 °C. It has been shown that $Fe_4N$ is the main phase (85 and 93 wt. %) of the steel surface layer after nitriding at 520 and 600 °C; a solid solution based on α- Fe is the main phase (97 wt. %) at lower temperatures. It has been found that the microhardness of the steel surface layer increases with the increase in the nitriding temperature and correlates with the relative content of the nitride phase. It has been shown that the maximum microhardness is recorded on the nitriding surfaces at nitriding temperatures 450 °C and 600 °C; in the subsurface layer at the depth of ~10 μm at nitriding temperature 520 °C. The greatest thickness

of the hardened layer (up to 500 μm) has been achieved after nitriding at 520 °C. It has been found that steel samples nitrided at 520 °C have relatively high wear, which is primarily due to the presence of micropores, which contribute to the embrittlement of the material.

**Acknowledgements**

The reported study was funded by RFBR and ROSATOM according to the research project No. 20-21-00111.

**5. References**

[1] Mirhosseini S.S., Mahboubi F., *Surface and Coatings Technology*, **435**, 128216, 2022; doi: 10.1016/j.surfcoat.2022.128216
[2] Hovsepian P., Shukla K., Sugumaran A., et al., *Materials Letters*, **313**, 131782, 2022; doi: 10.1016/j.matlet.2022.131782
[3] Naeem M., et al., *Journal of Building Engineering*, **47**, 103882, 2022; doi: 10.1016/j.jobe.2021.103882
[4] Budilov V.V., Agzamov R.D., Ramazanov K.N., *Metal Science and Heat Treatment*, **49**(7–8), 358, 2007; doi: 10.1007/s11041-007-0065-y
[5] Koval N.N., Ryabchikov A.I., Sivin D.O., et al., *Surface and Coatings Technology*, **34**, 152, 2018; doi: 10.1016/j.surfcoat.2018.02.064
[6] Lopatin I.V., Akhmadeev Yu.H., Koval N.N., Petrikova E.A., *IOP Conf. Series: Journal of Physics: Conf. Series*, **1115**, 032042, 2018; doi: 10.1088/1742-6596/1115/3/032042
[7] Sunghwan Yeo, et al., *Applied Surface Science*, **579**, 152133, 2022; doi: 10.1016/j.apsusc.2021.152133
[8] Godec M., Ruiz-Zepeda F., Podgornik B., et al., *Surface and Coatings Technology*, **433**, 128089, 2022; doi: 10.1016/j.surfcoat.2022.128089
[9] Meletis E.I., *Surface and Coatings Technology*, **149**(2–3), 95, 2002; doi: 10.1016/S0257-8972(01)01441-4
[10] Wei R., Benn C.R., Cooper C.V., *Plasma Process. Polym.*, **4**(1), 700, 2007; doi: 10.1002/ppap.200731801
[11] Akhmadeev Y.H., Ivanov Y.F., Krysina O.V., et al., *High Temperature Material Processes*, **25**(1), 47, 2021; doi: 10.1615/HighTempMatProc.2021038031
[12] Ivanov Y., Lopatin I., Denisova Y., et al., *Proc. 7th International Congress on Energy Fluxes and Radiation Effects, EFRE 2020*, 783, 2020; doi: 10.1109/EFRE47760.2020.9241927
[13] Lopatin I.V., Akhmadeev Yu.H., Koval N.N., *Review of Scientific Instruments*, **86**, 103301, 2015; doi: 10.1063/1.4932543
[14] Lopatin I.V., Akhmadeev Yu.H., Koval N.N., Kovalsky S.S., *Journal of Physics: Conference Series*, **1393**, 012046, 2019; doi: 10.1088/1742-6596/1393/1/012046
[15] Lopatin I.V., Akhmadeev Yu.H., Kovalsky S.S., Ignatov D.Yu., *Journal of Physics: Conference Series*, **2064**(1), 012029, 2021; doi: 10.1088/1742-6596/2064/1/012029